ARCHIVE OF MECHANICAL ENGINEERING

DOI: 10.24425/ame.2023.145584 2023, Vol. 70, No. 2, pp. 311–328

Dung Van NGUYEN [1], Viet Quy BUI [1], Dung Thai NGUYEN [1], Quyen Si UONG [1], Hieu Tu TRUONG [1]

Studying the thermo-gas-dynamic process in a muzzle brake compensator

Received 15 April 2023, **Revised** 19 May 2023, **Accepted** 23 May 2023, **Published online** 23 June 2023

Keywords: thermo-gas-dynamic, muzzle device, muzzle brake compensator, automatic gun

To reduce the recoil and improve the stability of small arms, a muzzle brake compensator is attached to the muzzle of the barrel. This device uses the kinetic energy of the powder gas escaping from the bore after the bullet is fired. In this paper, the authors present the determination of the thermo-gas-dynamic model of the operation of a muzzle brake compensator and an example of calculating this type of muzzle device for the AK assault rifle using 7.62×39 mm ammunition. The results of the calculation allowed for obtaining the parameters of the powder gas flow in the process of flowing out of the muzzle device, as well as the change in the momentum of the powder gas's impact on the muzzle device. The model proposed in the article provides the basis for a quantitative evaluation of the effectiveness of using the muzzle device in stabilizing infantry weapons when firing.

1. Introduction

Stability has a very significant effect on the dispersion of bullets and affects the firing efficiency of automatic weapons. It is crucial for ensuring the accuracy of serial firing from automatic hand-held weapons [1]. However, under the action of the forces and impulses that appear when firing, the weapon receives a backward motion, vibrating in both the vertical and horizontal planes, which determines the variability of the initial launch angle and direction. Therefore, there have been many studies to establish the model and investigate the influence of the basic factors on

✉ Viet Quy BUI, e-mail: vietbui.mta@gmail.com

[1]Faculty of Special Equipment, Le Quy Don Technical University, Hanoi, Vietnam. ORCIDs: D.V.N. 0000-0002-2810-1204; V.Q.B. 0009-0008-4844-124X; D.T.N. 0000-0003-3702-1692; Q.S.U. 0000-0001-9394-9212; H.T.T. 0000-0001-8414-8456

the stability of guns when shooting [2–9]. In order to reduce recoil and vibration without violating the firing mode and reduce the bullet velocity, many methods have been proposed to increase the stability of the gun [3, 5]. In addition to that, it has been found that a portion of the propellant energy is not converted into kinetic energy of the bullet and other work, but is retained in the powder gas released from the muzzle, which usually accounts for more than 40% of the total energy [10]. Thus, a research has been carried out on increasing the stability of the gun by using a muzzle device that takes advantage of this gaseous energy [11–20].

The muzzle device is a part or device arranged at the muzzle of the barrel, working in the final effect period of powder gas. It does not reduce the ballistic characteristics; in addition, it is simple in construction and has high reliability [21]. In the documents of weapon design calculations according to the thermodynamic principle of Kirillov [22] or the aerodynamic principle of Kulagin [23], the authors examined how the muzzle device affects the change in recoil momentum when firing, derived from the momentum balance equation of the "barrel – powder gas – bullet" system. From this, it can be seen that, for a given ballistic weapon, it is possible to influence the recoil momentum by changing the momentum of the muzzle device's impact on the system. To evaluate the efficiency of the muzzle device, two main characteristics are used: the energy efficiency factor ΔE, also known as the energy characteristic, and the impulse efficiency factor α_H, known as the structural characteristic. To determine the characteristic values of the muzzle device, it is necessary to solve the problem of the gas dynamics of the powder gas flow out of the combustion chamber limited by the bore, with the constant or abrupt expansion of the flow and partial loss through the side channels of the muzzle device. In this case, the basic equations of gas dynamics are used (conservation of energy, flow, and momentum), and the initial conditions (the powder gas parameters at the muzzle cross section) are found from the solution of the main problem of internal ballistics. Errors, which are inevitable in this case, can be compensated by proposing known fit coefficients from empirical studies of a given muzzle design scheme. Due to the use of a large number of experimental coefficients, it is not possible to accurately describe all the processes occurring for the typical muzzle device.

The need to further improve the efficiency of the muzzle device system has led to the emergence of new designs that differ from the traditional ones, therefore, the calculation of each particular design option will have its characteristics. An approach to modeling the operation of the muzzle device was considered using ANSYS CFX and an example was calculated for the muzzle device of the 152 mm 2A36 cannon. The boundary conditions, pressure, temperature, and velocity of the powder gas at the inlet of the muzzle brake were obtained from the results of the internal ballistics problem. The projectile is assumed to travel at a constant speed, corresponding to the speed of the projectile at the muzzle. The obtained results were the parameters of the gas flow in the process of flowing out of the muzzle device as well as the graph of the change in the pulling force of the muzzle device [11]. On the other hand, gas-dynamic models of the muzzle device have been simulated, such as a model to investigate its influence on sabot separation [12] or a model to

calculate the rotation and braking force of the muzzle device for a Gatling gun [13]. Studying the characteristics of the silencer and the nature of thermodynamic processes in the chambers of this device, Konovalov and colleagues introduced a way to calculate the gas flow in the chambers of the silencer closer to the real flow, and considerations were made regarding the physical phenomena that need to be studied to clarify the main properties. The authors suggested that the gas parameters in each chamber during the entire time from when the bullet entered the device to the time it left were constant in terms of chamber volume but varied with time. The gas velocity in the center tube is equal to the bullet velocity; in the chambers, it is taken to be zero. To calculate the parameters of a non-stationary process, a system of ordinary differential equations is used based on applying the conservation laws of mass and energy to the volume of gas in each chamber of the device, taking into account gas flow through the holes in the walls of the chambers [14]. Patrikova introduced a mathematical model of the muzzle device on non-lethal weapons with deformable bullets. The author also conducted experiments to evaluate the calculation error. The qualitative results do not contradict the physical model of the phenomena under consideration, and the quantitative results agree satisfactorily with the experimental results [15]. If the weapon attaching a muzzle brake is fired, complex jet flows are ejected from the small-caliber gun, and the muzzle waves have arguably more severe effects. Therefore, a simulation model calculated the muzzle gas flows and the acoustic noise for the case with and without the muzzle brake, and then a comparison between them was performed to predict the noise effect and optimize the structure of muzzle brakes [16]. Alternatively, a model analyzed the influence of the muzzle brake structure on chemical reactions, the interaction of blast waves, and the formation mechanism of muzzle flash, providing a reference for researchers studying muzzle flash suppressions [17]. To evaluate the effectiveness of the muzzle brake, numerical investigations of the firing process with different muzzle brake devices were carried out in a quasi-realistic situation [18]. Besides, numerical experiments were performed on a gun with a muzzle gas dynamic device, a perforated barrel brake, based on simultaneous consideration of the problem of internal and intermediate ballistics [19]. The results of the mathematical models are consistent with the data from natural experiments.

For automatic firearms, studies have shown that a single-function muzzle device will not be able to guarantee stable conditions for the gun. Therefore, in order to improve the stability of the gun when shooting, the current general trend is using a gas compensator combined with a recoil brake [22]. The effect of the muzzle brake compensator on the stability of automatic hand-held weapons when firing in series was investigated in an experiment [20]. The author has given the results of the pressure force on the barrel bottom during the final effect period, the backward length of the shoulder rest, and the barrel bounce angle in the vertical and horizontal planes and compared them with the case without the muzzle device. However, the dynamic process in the device has not been fully considered by the author. Accordingly, this article will introduce a thermo-gas-dynamic model to calculate the operation process of the muzzle brake compensator.

2. Thermo-gas-dynamic model of powder gas in the muzzle brake compensator

2.1. Basic assumptions

The thermo-gas-dynamic problem of the muzzle device during its operation is one of the complex problems and is solved based on solving the equations defining the parameters of the powder gas state, which depend on the flow shape and the heat exchange conditions with the outside environment. When constructing the calculating equations, it is necessary to use the following additional assumptions:

a) The propellant burns out in the bore before the bullet moves to the muzzle of the barrel;
b) Filling the working cavities of the muzzle device with powder gas is carried out instantly, and the powder gas flows out from the space behind the bullet through the clearance between the bullet and the bore at the inlet section in the critical mode;
c) The outflow of powder gas from the working chambers of the muzzle device is in critical mode during the entire final effect period;
d) The calculation of the powder gas flow in the muzzle device in the areas of smooth and sudden extensions and lateral discharge into the atmosphere are carried out according to the established relationships [22–24] taking into account the direct impact caused by the deceleration of the supersonic flow in the working cavity in the presence of a baffle and the influence of the oblique cut on the outlet parts of the exhaust channels.

2.2. Model for calculations

The structure of a two-chamber muzzle device has a cylindrical shape with compensation holes on the wall of the first chamber and windows in the second chamber, as shown in Fig. 1.

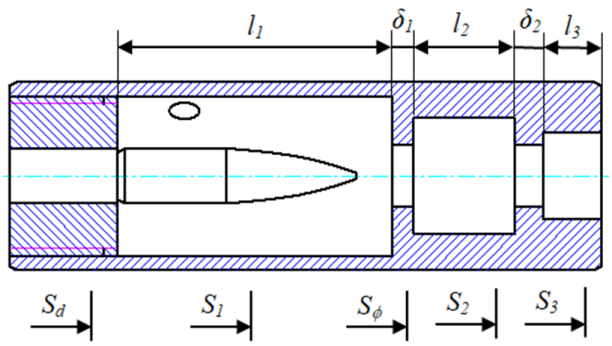

Fig. 1. Diagram of a muzzle brake compensator

It can be seen that the powder gas moving through the muzzle from the bore flows into the first chamber of the device at the speed of sound. After that, the sound stream expands, its speed increases rapidly and becomes supersonic. The subsequent movement of the gas in the cavity is determined by the passage of the gas through the hole to the second chamber and the lateral holes. Under the influence of gas outflow through the holes, the supersonic flow velocity continues to increase. Due to the presence of an anterior reflective baffle in the cavity, a direct impact occurs, converting the supersonic flow into a subsonic flow and dividing the cavity into two zones: the supersonic flow area and the subsonic flow area. When the bullet moves to the hole between the two chambers, the subsonic speed of the gas flow decreases and the pressure and temperature of the gas both increase. Under the action of the total pressure in front of the reflecting baffle, the gas flow from the first chamber enters the second chamber at the speed of sound at the narrowest cross-section of the stream. The process is similar to that in the first chamber.

2.3. Descriptive equations

The mathematical model includes the following groups of equations. The equations for the change in mass and internal energy of the gas in the first chamber:

$$\frac{\mathrm{d}m_1}{\mathrm{d}t} = G_d - G_{12} - G_{1\phi}\,, \tag{1}$$

$$\frac{\mathrm{d}U_1}{\mathrm{d}t} = H_0 G_d - H_1\left(G_{12} + G_{1\phi}\right) - \frac{\mathrm{d}Q_1}{\mathrm{d}t}\,, \tag{2}$$

where m_1 and U_1 are the mass and internal energy of the gas in the first chamber; G_d, G_{12}, $G_{1\phi}$ indicate gas flow rates from bore to the first chamber, from the first chamber to the second chamber and from the first chamber through side holes into the atmosphere, respectively; H_0, H_1 are gas energies for specific flows; Q_1 is energy loss of the gas in the first chamber due to heat transfer.

The equations for the change in mass and internal energy of the gas in the second cavity:

$$\frac{\mathrm{d}m_2}{\mathrm{d}t} = G_{12} - G_{2d} - G_{2\Delta}\,, \tag{3}$$

$$\frac{\mathrm{d}U_2}{\mathrm{d}t} = H_1 G_{12} - H_2\left(G_{2d} + G_{2\Delta}\right) - \frac{\mathrm{d}Q_2}{\mathrm{d}t}\,, \tag{4}$$

where G_{2d} and $G_{2\Delta}$ are gas flow rates from the second chamber through the front hole and brake windows, respectively, into the atmosphere.

The equation for determining the energy loss of the powder gas due to heat transfer:

$$\frac{\mathrm{d}Q_i}{\mathrm{d}t} = \alpha_i \frac{\left(T_i - T_n\right) F_i - \dfrac{4}{3\sqrt{\pi}v_\tau}\dfrac{Q_i}{\sqrt{t - t_d}}}{1 + \alpha_i \dfrac{2}{3\sqrt{\pi}v_\tau}\sqrt{t - t_d}}\,. \tag{5}$$

In this formula, T_n is the initial internal surface temperature of the device; T_i is the temperature of the powder gas in the chamber i; ν_τ is the heat absorption coefficient of the material; F_i is the heat transfer surface area of the chambers; t_d is the time taken by the bullet traveling to the muzzle section; α_i is the heat transfer coefficient.

Equation of gas energy for specific flows:

$$H_i = \frac{k}{k-1} RT_i \,, \tag{6}$$

where k is the heat capacity ratio of the powder gas, and R is the gas constant.

Equations for gas flow rates:

$$G_d = \begin{cases} \mu_d F_d B(k) \dfrac{p_d}{\sqrt{RT_d}} \sqrt{1 - \left(\dfrac{p_1}{p_d}\right)^2} & \text{when } p_d \geqslant p_1 \,, \\ 0 & \text{when } p_d < p_1 \,, \end{cases} \tag{7}$$

$$G_{12} = \begin{cases} \mu_{12} F_{12} B(k) \dfrac{p_1}{\sqrt{RT_1}} \sqrt{1 - \left(\dfrac{p_2}{p_1}\right)^2} & \text{when } p_1 \geqslant p_2 \,, \\ 0 & \text{when } p_1 < p_2 \,, \end{cases} \tag{8}$$

$$G_{1\phi} = \mu_{1\phi} F_{1\phi} B(k) \frac{p_1}{\sqrt{RT_1}} \sqrt{1 - \left(\frac{p_a}{p_1}\right)^2} \,, \tag{9}$$

$$G_{2d} = \mu_{2d} F_{2d} B(k) \frac{p_2}{\sqrt{RT_2}} \sqrt{1 - \left(\frac{p_a}{p_2}\right)^2} \,, \tag{10}$$

$$G_{2\Delta} = \mu_{2\Delta} F_{2\Delta} B(k) \frac{p_2}{\sqrt{RT_2}} \sqrt{1 - \left(\frac{p_a}{p_2}\right)^2} \,, \tag{11}$$

with $B(k) = \left(\dfrac{2}{k+1}\right)^{\frac{k+1}{2(k-1)}} \sqrt{k}$.

In the above equations, F_{ij} is the cross-sectional area of the gas flows; p_d, p_1, p_2, p_a are the powder gas pressure at the muzzle, gas pressure in the first and second chamber and the barometric pressure; μ_{ij} indicates the flow coefficient, which depends on the duct geometry and the dimensionless velocity of the gas.

The flow coefficient is a function of the duct geometry and the dimensionless velocity of the gas [25]:

$$\mu = \varphi_v \varepsilon_m \,, \tag{12}$$

where φ_v is the coefficient of velocity, due to the viscosity of the gas and taking into account the uneven distribution of the velocity in the narrow part of the gas duct, approximately equal to 0.97; ε_m is the maximum value of the duct narrowing coefficient, which is determined by the formula in [26]:

$$\varepsilon_m = \varepsilon_n \left[k - (k-1)\varepsilon_n\right]^{\frac{1}{k-1}} . \tag{13}$$

In this formula, ε_n is the narrowing coefficient of an incompressible liquid, depending on the input geometry of the sections:

$$\varepsilon_n = \frac{1}{1 + \dfrac{1-\varepsilon_{n0}}{\varepsilon_{n0}} e^{\frac{8r}{d}} \sqrt{1 - \left(\dfrac{F_2}{F_1}\right)^2}} \,, \tag{14}$$

where ε_{n0} is the narrowing coefficient of the incompressible liquid as it exits an infinitely wide vessel ($F_2/F_1 = 0$):

$$\varepsilon_{n0} = \frac{\pi}{\pi + a} \,. \tag{15}$$

There, $a = \displaystyle\int_0^{\pi} \cot\frac{x}{2} \sin\left(\frac{\theta}{180}x\right) \mathrm{d}x$; θ is the inclined angle of the gas outlet and the barrel axis.

In the case of powder gas flow moving into the device and flowing through the side hole of the device wall, the flow coefficient is determined [24]:

$$\mu_s = 0.97 \frac{\sqrt{\tau(\lambda_1)}}{\pi(\lambda_1)} \varepsilon_{mb} = \left(1 - \frac{\Omega(\lambda_2)}{\Omega(\lambda_1)}\right) y(\lambda_1) \sqrt{\tau(\lambda_1)} \frac{S}{F} \,, \tag{16}$$

where S is the cross-sectional area of the device; F is the cross-sectional area of the hole; λ_1 is the dimensionless velocity of powder gas flow at the gas port; λ_2 is the dimensionless velocity of gas flow after extracting, is determined:

$$\Phi(\varphi, \lambda_2) = \Phi(\varphi, \lambda_1) - \frac{S}{F} \,. \tag{17}$$

The values of the aerodynamic functions $y(\lambda)$, $\tau(\lambda)$, $\Omega(\lambda)$ and $\Phi(\lambda)$ are taken from the appendix table [24].

The equations for the gas state parameters in the chambers:

$$p_i = (k-1)\frac{U_i}{W_i}, \tag{18}$$

$$T_i = \frac{k-1}{R}\frac{U_i}{m_i}. \tag{19}$$

The equations for the heat transfer coefficients are:

$$\alpha_1 = \frac{42}{W_1^{0.55}}\left[G_d^{0.65} + 3.1\left(G_{12} + G_{1\phi}\right)^{0.65}\right], \tag{20}$$

$$\alpha_2 = \frac{42}{W_2^{0.55}}\left[G_{12}^{0.65} + 3.1\left(G_{2d} + G_{2\Delta}\right)^{0.65}\right]. \tag{21}$$

The equation for changing the volume of the gas chambers:

$$W_i = W_{i0} + F_{bb}V(l), \tag{22}$$

where W_{i0} is the initial volume of the chamber considering the bullet volume; F_{bb} is the bottom area of the bullet; $V(l)$ is the bullet velocity.

The system of equations is solved in combination with the equations system of internal ballistics. The integral of differential equations will stop when there is a decrease in the pressure in the gas chambers to atmospheric pressure.

3. The thermo-gas-dynamic process in the muzzle brake compensator of the AK assault rifle

3.1. Initial data

The thermo-gas-dynamic process in the muzzle brake compensator attached to the 7.62 mm AKM assault rifle using 7.62×39 mm ammunition was investigated. The initial structural parameters and others necessary for the calculation are summarized in Table 1 and Table 2.

Table 1. Ballistics data

Parameter	Value	Parameter	Value	Parameter	Value
d (m)	7.62×10^{-3}	q (kg)	0.0079	b (m^3/kg)	0.995×10^{-3}
d_d (m)	7.92×10^{-3}	ω (kg)	0.0016	χ	1.06
W_0 (m^3)	2.18×10^{-6}	P_0 (N/m^2)	4×10^6	$\chi\lambda$	–0.06
l_0 (m)	0.065	f (Nm/kg)	98×10^3	θ	0.2
S (m^2)	45.6×10^{-6}	I_k (Ns/m^2)	1275×10^4	c_k	1.252
l_d (m)	0.386	α (m^3/N)	10^{-4}	p_a (N/m^2)	1.01×10^5
l_ϕ (m)	0.270	δ (N/m^3)	1.6×10^4		

Table 2. Parameters of the muzzle device

Parameter	Value	Parameter	Value	Parameter	Value
d_1 (m)	22×10^{-3}	δ_{12} (m)	3×10^{-3}	φ_1 (°)	40
d_1 (m)	38×10^{-3}	d_3 (m)	12×10^{-3}	φ_2 (°)	30
d_2 (m)	16×10^{-3}	δ_{23} (m)	4×10^{-3}	φ_3 (°)	90
l_2 (m)	14×10^{-3}	d_{ex} (m)	26×10^{-3}	α_Δ (°)	34
d_{12} (m)	8×10^{-3}	φ (m)	4×10^{-3}		
λ_τ (W/m K)	46.1	a_τ (m/s^2)	1.2×10^{-5}		

3.2. Results

The results are presented graphically in Fig. 2 to Fig. 6, describing the temporal distribution of the main gas parameters in the chambers of the muzzle brake compensator. The following key parameters are given: time-varying curves of pressure (Fig. 2), temperature (Fig. 3), gas mass (Fig. 4), gas flow (Fig. 5) and force produced by the powder gas acting on the gun during the final period of effect (Fig. 6).

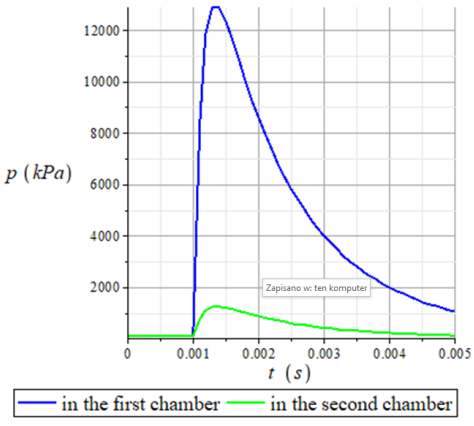

Fig. 2. Graph of pressure curve in two device chambers over time

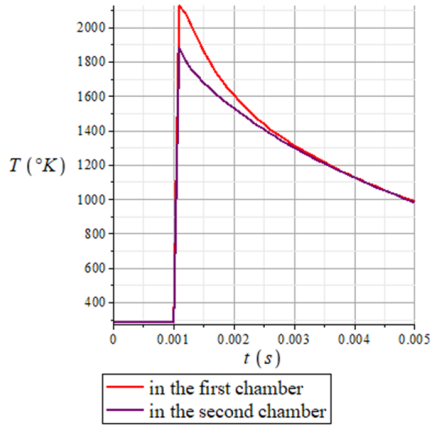

Fig. 3. Graph of gas temperature change in two device chambers over time

As can be seen in Fig. 2, the pressure in the first chamber of the muzzle device increases sharply, indicating that at this moment the bottom of the bullet has reached the device channel cross-section. The increase in pressure in the second chamber of the device indicates the ingress of gas into it at the appropriate time.

On the graph of the temperature distribution in the chambers of the device (Fig. 3), one can observe a rapid increase in the temperature of the gas flow during its deceleration by the bullet and the walls of the chambers and the subsequent turn of the gas in the direction of the slots of the muzzle device. The temperature drops in the cavities are associated with pronounced dynamics of the flow process.

Graphs of changing mass of the gas and gas flow clearly show the operation of each muzzle brake compensator chamber (Fig. 4 and Fig. 5). The greater consumption of mass of the gas in the device is carried out in the first compartment (close to the muzzle) and smaller – in the second.

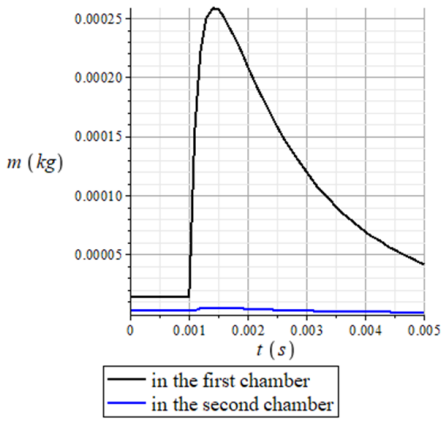

Fig. 4. Graph of gas mass change in two device chambers over time

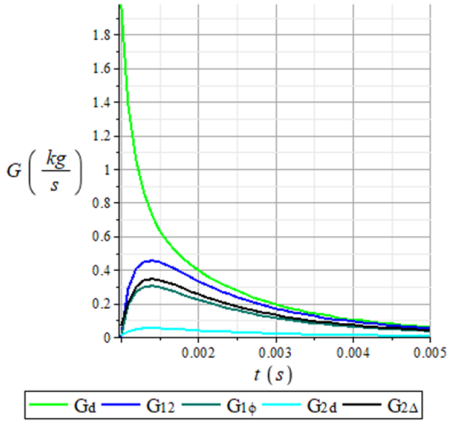

Fig. 5. Graph of gas flows change in muzzle device over time

The force graph clearly shows the working effect of the muzzle brake compensator (Fig. 6). Negative thrust values indicate the generation of forces opposite to the direction of gun motion. Due to the effect of the muzzle device, the bottom barrel force of the gas pressure during the final effect period when using the muzzle brake compensator is smaller than when the device is not available. It is this reduction in the momentum applied to the gun along the barrel axis combined with

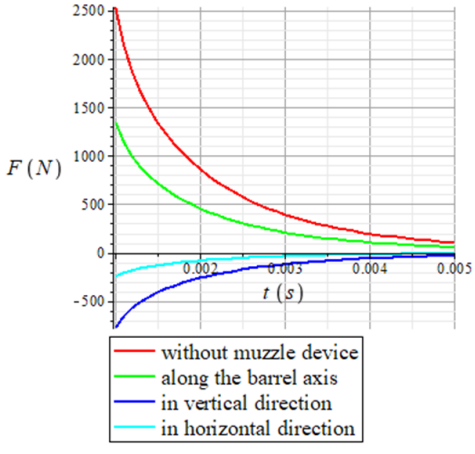

Fig. 6. Graph of forces change of gas in the final effect period in two cases: without muzzle device and with muzzle device

the force generated by the side gas flows, which greatly improves the stability of the gun when firing. Figs. 7 and 8 compare the results of gun dynamics in serial firing with and without the device. The coefficient of effectiveness of the muzzle device of the considered design during the departure of the bullet is about 47%.

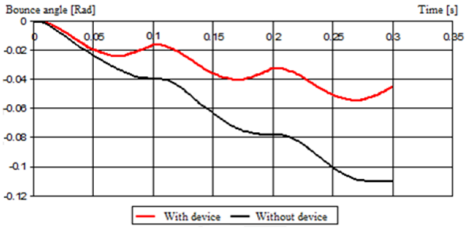

Fig. 7. Bounce angle of the gun barrel in the vertical plane in two cases: without muzzle device and with muzzle device

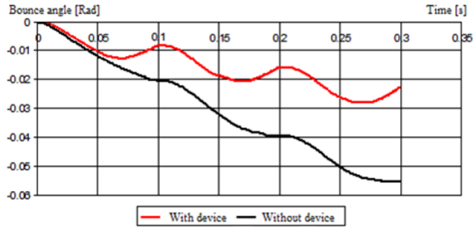

Fig. 8. Bounce angle of the gun barrel in the horizontal plane in two cases: without muzzle device and with muzzle device

The two-chamber design of the muzzle device is loaded by the pressure of powder gas unevenly. A greater load is the first chamber and a lower load is the second chamber. The average distribution of high-velocity flow and temperature over the volume of all chambers of the device as the bullet leaves the device is approximately the same.

4. Experiment

4.1. Structural model and arrangement of measuring positions on the gun

The experiment was conducted in the firing cellar of the Experimental Center of Weapons at Le Quy Don Technical University, Vietnam.

The experimental equipment structure includes an AKM assault rifle mounted on a specialized rack with a reverse block and links to limit errors due to the gunner's manipulation while ensuring the most realistic description of normal firing conditions. The gun is fired by an indirect trigger puller, ensuring that the trigger force is the internal force (for the gun), thus completely eliminating the unwanted effects of the shooter on the gun (Figs. 9 and 10). The muzzle device is attached to the gun when firing, as shown in Fig. 11.

The structural parameters of the rack and the oscillating frame are as follows: the rack dimensions (length × width × height) are 900 × 250 × 760 mm, weight is 94 kg; the reverse block mass is 20 kg; the stiffness of the reverse block spring is 1600 N/m; and the spring stiffness on the oscillating frame is 55 N/m. Fig. 12 shows a block diagram describing the experimental system to determine the dynamic parameters (in the firing plane).

In the diagram of Fig. 12, the measuring object is in the standard state, the DATRON displacement probe body is fixed on the probe mount and does not move

Fig. 9. Experimental setup

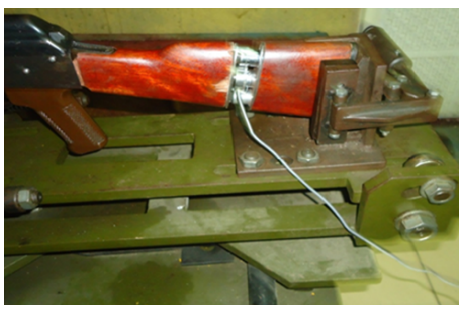

Fig. 10. Recoil force measuring jig

Fig. 11. Experimental muzzle device

when fired, and the reflector mounted on the barrel tip moves with the gun body. The piezoelectric sensor is located at the gun stock position to determine the axial recoil force of the gun. The measured signal is sent to the DEWETRON 3000 dynamic signal analyzer. The displacement in two vertical planes (the firing plane) and the horizontal plane is measured, on that basis one determines the bounce angle of the gun when firing.

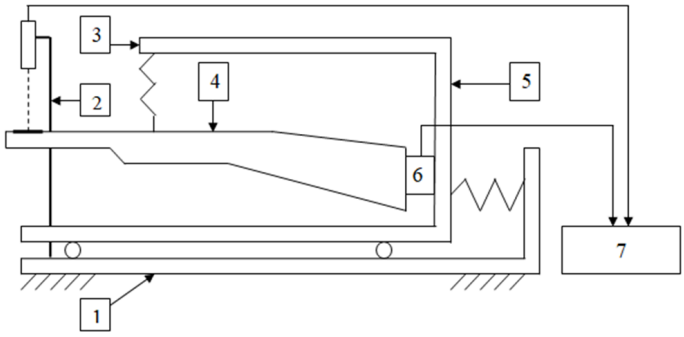

Fig. 12. The block diagram of the test system: 1 fixed specialized rack; 2 mounting bracket and displacement sensor; 3 front mount for gun and spring; 4 measuring object (AKM gun); 5 reverse block and spring; 6 piezoelectric sensor; 7 signal analyzer and display device

4.2. Experimental results

In accordance with the test plan described above, the test carried out measurements for the variants with and without the muzzle device. The graph of the vertical and horizontal displacement measurement results in the first measurement is shown in Figs. 13 to 16.

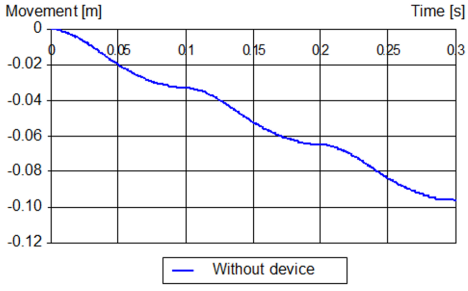

Fig. 13. Bounce angle of the gun without the muzzle device in the vertical plane

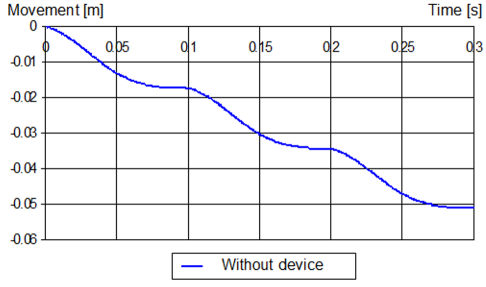

Fig. 14. Bounce angle of the gun without the muzzle device in the horizontal plane

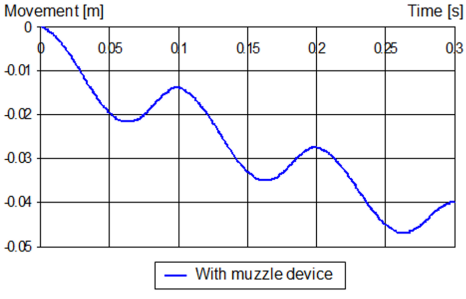

Fig. 15. Bounce angle of the gun with the muzzle device in the vertical plane

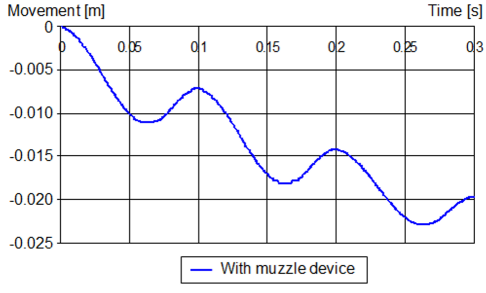

Fig. 16. Bounce angle of the gun with the muzzle device in the horizontal plane

From the results of theoretical calculations and experimental results, after being processed and evaluated for errors, tables are made to compare the theoretical and experimental results with the vertical and horizontal bounce angle results at the end of each shot in the series (Tables 3 and 4).

Table 3. Comparison of theoretical and experimental results for vertical bounce angle

Option	End of 1st shot			End of 2nd shot			End of 3rd shot		
	Theoretical result (rad)	Experimental result (rad)	Error (%)	Theoretical result (rad)	Experimental result (rad)	Error (%)	Theoretical result (rad)	Experimental result (rad)	Error (%)
without muzzle device	0.03936	0.0369	6.7	0.07783	0.0728	6.9	0.1103	0.1084	1.8
with muzzle device	0.0164	0.0153	7.2	0.032	0.0303	5.6	0.045	0.0446	1

Table 4. Comparison of theoretical and experimental results for horizontal bounce angle

Option	End of 1st shot			End of 2nd shot			End of 3rd shot		
	Theoretical result (rad)	Experimental result (rad)	Error (%)	Theoretical result (rad)	Experimental result (rad)	Error (%)	Theoretical result (rad)	Experimental result (rad)	Error (%)
without muzzle device	0.02047	0.0191	7.2	0.03935	0.0376	4.7	0.05515	0.056	1.5
with muzzle device	0.00856	0.0079	8.4	0.0162	0.0156	3.8	0.0223	0.022	1.4

The result of measuring the recoil force when firing a series of three rounds on the rack is shown in Fig. 17.

According to the parameters of the measuring system with 1 mV/s = 30 N, we have the conversion results as in Table 5.

Table 5. Impulse acting on the stock when firing a series of 3 rounds

Shot times / Impulse (N s)	1st	2nd	3rd	4th	5th	Average value
without muzzle device	2.625	2.607	2.754	2.559	2.355	2.58
with muzzle device	1.968	1.955	2.093	1.945	1.813	1.955

The intermediate deviation of the dispersion of the gun installed with the muzzle brake compensator was determined when shooting the series of three rounds, number of series 50, in a lying position with a pedestal. From the distribution of the bullet's impact points shown in Fig. 18, the intermediate deviations typical for

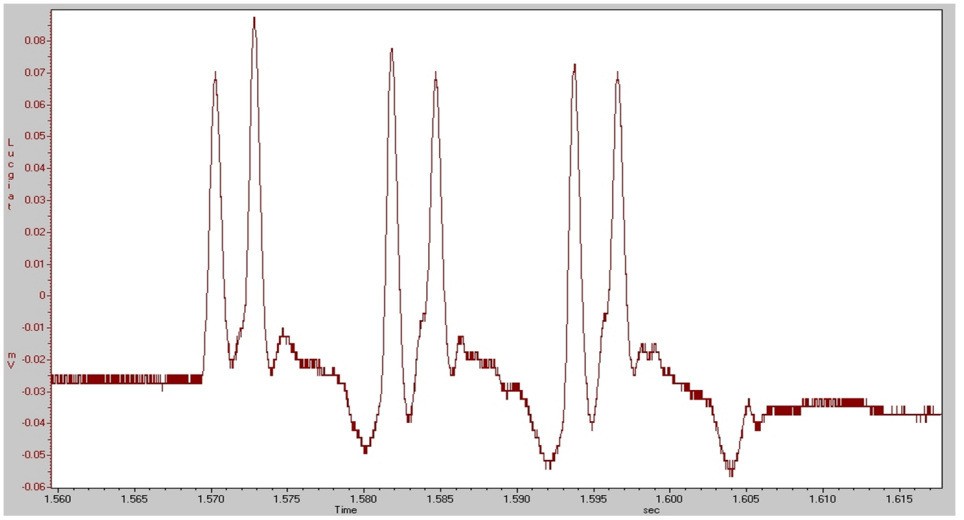

Fig. 17. Graph of the result of measuring the recoil force of the 3-shot series

the dispersion of the bullets when firing in series are determined by height and direction $L_{H^r} = 0.143$ m, $L_{D^r} = 0.165$ m. The corresponding values of the tables of shooting are $L_{H^t} = 0.21$ m, $L_{D^t} = 0.24$ m.

Fig. 18. Bullet impact point distribution

4.3. Comment on experimental results and comparison with theoretical calculations

The experimental results are in agreement with the theoretical calculation results. With the measurements for each dynamic parameter of the whole series of shots, we obtained the value of the different average bounce angle of the gun body

at the end of each shot and the different forces acting on the gunner's shoulder. Those results do not differ much compared with theoretical calculation results (the error of bounce angle ranges from 1% to 8.4%, the error of recoil force is 9.47%). This proves that the established model is correct.

The result of comparing the intermediate deviations that characterize the dispersion of bullets when firing in series confirms once again the effectiveness of the muzzle device on the improvement of accuracy of the gun during firing a short series.

5. Conclusions

A complex physical and mathematical model of the dynamical process that occurs inside a muzzle device of automatic guns has been presented in this paper. Calculation of the gas flow process in the muzzle device is carried out simultaneously with the internal ballistics problem and the process in the gas engine based on Maple software. As a result of the calculations, the following was established:

- The process of the gas flow in the barrel, the gas chamber and the muzzle device has a pronounced non-stationary and essentially non-linear turbulent character;
- When the gas flow interacts with the chambers of the muzzle device, the flow and its turn decelerate quickly, resulting in a sharp increase in the temperature in the chambers and the appearance of intense gas flows with high mass flow escaping through the holes on the muzzle device;
- In multi-chamber design of the muzzle device, the function of each chamber is different. The first chamber of the muzzle brake compensator makes the greatest contribution to the generation of anti-recoil and compensatory force, the subsequent chamber makes a smaller contribution than the previous one.
- The recoil does not begin to appear when the bullet leaves the muzzle, but when the bullet begins to move in the initial phase of the shot. On light rifles, it is completely impossible to eliminate the recoil momentum with the help of a muzzle device, and the recoil at the beginning of the shot will always be present. However, due to the effect of the muzzle brake compensator, the gun's stability is significantly improved up to the time of the start of the second shot in the shots series.

The model proposed in this article provides the basis for a quantitative evaluation of the effectiveness of using the muzzle device in stabilizing firearms when firing.

References

[1] V.V. Alferov. *Design and Calculation of Automatic Weapons*. Moscow, Mechanical Engineering, 1977 (in Russian).

[2] M. Stiavnicky and P. Lisy. Influence of barrel vibration on the barrel muzzle position at the moment when bullet exits barrel. *Advances in Military Technology*, 8(1):89–102, 2013.

[3] D.M. Hung. *Study on the dynamics of the AGS-17 30mm grenade launcher and the effect of some structural factors on gun stability when fired*. PhD Thesis, Military Technical Academy, Hanoi, 2016 (in Vietnamese).

[4] J. Balla. Contribution to determining of load generated by shooting from automatic weapons. *International Conference on Military Technologies (ICMT)*, pages 1–6, Brno, Czech Republic, 30-31 May 2019. doi: 10.1109/MILTECHS.2019.8870116.

[5] V.B. Vo, J. Balla, H.M. Dao, H.T. Truong, D.V. Nguyen, and T.V. Tran. Firing stability of automatic grenade launcher mounted on tripod. *International Conference on Military Technologies (ICMT)*, pages 1–8, Brno, Czech Republic, August 2021. doi: 10.1109/ICMT52455.2021.9502836.

[6] M. Macko, B.V. Vo, and Q.A. Mai. Dynamics of short recoil-operated weapon. *Problems of Mechatronics. Armament, Aviation, Safety Engineering*, 12(3):9–26, 2021. doi: 10.5604/01.3001.0015.2432.

[7] N.T. Dung, N.V. Dung, T.V. Phuc, and D.D. Linh. biomechanical analysis of the shooter-weapon system oscillation. *International Conference on Military Technologies (ICMT)*, Brno, Czech Republic, pages 48–53, 2017. doi: 10.1109/MILTECHS.2017.7988729.

[8] V.B. Vo, M. Macko, and H.M. Dao. Experimental study of automatic weapon vibrations when burst firing. *Problems of Mechatronics. Armament, Aviation, Safety Engineering*, 12(4):9–28, 2012. doi: 10.5604/01.3001.0015.5984.

[9] T.D. Van, T.L. Minh, D.N. Thai, D.T. Cong, and P.V. Minh. The application of the design of the experiment to investigate the stability of special equipment. *Mathematical Problems in Engineering*, 2022: 8562602, 2022. doi: 10.1155/2022/8562602.

[10] Instructions on shooting. Gun shooting basics. 7.62 mm Modernized Kalashnikov assault rifle (AKM and AKMS), 7.62 mm Kalashnikov light machine gun (RPK and RPKS), 7.62 mm Kalashnikov machine gun (PK, PKS, PKB and PKT), 9 mm Makarov pistol. Hand grenades. *Military Publishing House of the USSR Ministry of Defense*, 1973 (in Russian).

[11] D.N. Zhukov, V.V. Chernov, and M.V. Zharkov. Development of an algorithm for calculating muzzle devices in the CFD package, Fundamentals of ballistic design. *All-Russian Scientific and Technical Conference*, St. Petersburg, pages 126-129, 2012. (in Russian).

[12] R. Cayzac, E. Carette, and T. Alziary de Roquefort. 3D unsteady intermediate ballistics modelling: Muzzle brake and sabot separation, In *Proceedings of the 24th International Symposium on Ballistics*, New Orleans, LA, USA, pages 423–430, 2008.

[13] J.S. Li, M. Qiu, Z.Q. Liao, D.P. Xian, and J. Song. Dynamic modeling and simulation of Gatling gun with muzzle assistant-rotating and recoil absorber. *Acta Armamentarii*, 35(9):1344–1349, 2014. doi: 10.3969/j.issn.1000-1093.2014.09.003.

[14] N.A. Konovalov, O.V. Pilipenko, Yu.A. Kvasha, G.A. Polyakov, A.D. Skorik, and V.I. Kovalenko. On thermo-gas-dynamic processes in devices for reducing the sound level of a small arms shot. *Technical Mechanics*, pp. 69-81, 2011 (in Russian).

[15] E.N. Patrikov. Mathematical modeling of the functioning process of service weapons in the mode of non-lethal action. *Technical Sciences, News of TulGU*, pp. 33-39, 2012 (in Russian).

[16] X.Y. Zhao, K.D. Zhou, L. He, Y. Lu, J. Wang, and Q. Zheng. Numerical simulation and experiment on impulse noise in a small caliber rifle with muzzle brake. *Shock and Vibration*, 2019: 5938034, 2019. doi: 10.1155/2019/5938034.

[17] P.F. Li and X.B. Zhang. Numerical research on adverse effect of muzzle flow formed by muzzle brake considering secondary combustion. *Defence Technology*, 17(4):1178–1189, 2021. doi: 10.1016/j.dt.2020.06.019.

[18] H.H. Zhang, Z.H. Chen, X.H. Jiang, and H.Zh. Li. Investigations on the exterior flow field and the efficiency of the muzzle brake. *Journal of Mechanical Science and Technology*, 27: 95–101, 2013. doi: 10.1007/s12206-012-1223-8.

[19] I. Semenov, P. Utkin, I. Akhmedyanov, I. Menshov, and P. Pasynkov. Numerical investigation of near-muzzle blast levels for perforated muzzle brake using high performance computing. *International Conference "Parallel and Distributed Computing Systems" PDCS 2013*, pages 281–289, Ukraine, Kharkiv, March 13-14, 2013. (in Russian).

[20] S.Q. Uong. Investigating the effect of gas compensator combined with brake device on the stability of automatic hand-held weapons when firing in series by experiment. *Military Technical and Technological Science Research*, 23:80–83, 2008. (in Vietnamese).

[21] L.E. Mikhailov. Designs of Small Automatic Arms Weapons. Central Research Institute of Information, USSR, 1984. (in Russian).

[22] *Theory and Calculation of Automatic Weapons*.V.M. Kirillov (editor). Penza: PVAIU, 1973. (in Russian).

[23] V.I. Kulagin and V.I. Cherezov. *Gas Dynamics of Automatic Weapons*. Central Research Institute of Information, USSR, 1985. (in Russian).

[24] Yu.P. Platonov. *Thermo-gas-dynamics of Automatic Weapons. Mechanical Engineering*, USSR, 2009. (in Russian).

[25] M.I. Gurevich. *Theory of Jets of an Ideal Fluid*. Fizmatgiz, USSR, 1961. (in Russian).

[26] Guiding Technical Material, Small Arms, Methods of Thermo-Gas-Dynamic Calculations. RTM-611-74, 1975. (in Russian).